Ultrafast recovery time and broadband saturable absorption properties of black phosphorus suspension

Yingwei Wang, Guanghui Huang, Haoran Mu, Shenghuang Lin, Jiazhang Chen, Si Xiao, Qiaoliang Bao, and Jun He

View Online   **Export Citation**   **CrossMark**

ARTICLES YOU MAY BE INTERESTED IN

Black phosphorus saturable absorber for ultrashort pulse generation
Applied Physics Letters 107, 051108 (2015); https://doi.org/10.1063/1.4927673

Carrier dynamics and transient photobleaching in thin layers of black phosphorus
Applied Physics Letters 107, 081103 (2015); https://doi.org/10.1063/1.4929403

Thermoelectric power of bulk black-phosphorus
Applied Physics Letters 106, 022102 (2015); https://doi.org/10.1063/1.4905636

Ultrafast recovery time and broadband saturable absorption properties of black phosphorus suspension

Yingwei Wang,[1] Guanghui Huang,[1] Haoran Mu,[2] Shenghuang Lin,[2,3] Jiazhang Chen,[1] Si Xiao,[1,a)] Qiaoliang Bao,[2] and Jun He[1,b)]

[1]*Institute of Super-Microstructure and Ultrafast Process in Advanced Materials, School of Physics and Electronics, Central South University, 932 South Lushan Road, Changsha, Hunan 410083, People's Republic of China*

[2]*Institute of Functional Nano and Soft Materials (FUNSOM), Jiangsu Key Laboratory for Carbon-Based Functional Materials and Devices, and Collaborative Innovation Center of Suzhou Nano Science and Technology, Soochow University, Suzhou 215123, People's Republic of China*

[3]*Department of Applied Physics, The Hong Kong Polytechnic University, Hung Hom, Hong Kong, China*

As a new type of two-dimensional crystal material, black phosphorus (BP) exhibits excellent electronics and optical performance. Herein, we focus on carrier relaxation dynamics and nonlinear optical properties of BP suspension. Atomic force microscopy, transmission electron microscopy, and optical transmission spectrum are employed to characterize the structure and linear optical properties of the BP. Additionally, pump-probe experiments at wavelength of 1550 nm were carried out to study the carrier dynamics in BP suspension, and ultrafast recovery time was observed ($\tau_s = 24 \pm 2$ fs). Furthermore, we demonstrate the saturable absorption signals by open aperture Z-scan experiments at wavelengths of 1550 nm, 532 nm, and 680 nm. The results indicate that BP has broadband saturable absorption properties and the nonlinear absorption coefficients were determined to be $\beta_2 = -0.20 \pm 0.08 \times 10^{-3}$ cm/GW (532 nm), $\beta_2 = -0.12 \pm 0.05 \times 10^{-3}$ cm/GW (680 nm), and $\beta_2 = -0.15 \pm 0.09 \times 10^{-3}$ cm/GW (1550 nm). © 2015 AIP Publishing LLC.
[http://dx.doi.org/10.1063/1.4930077]

Black phosphorus (BP) is a layered, phosphorus allotrope, two-dimensional (2D) crystal material. Just like graphitic structure, individual atomic layers are stacked together by Van Der Waals interactions in BP. Each phosphorus atom is bonded with three adjacent phosphorus atoms, but they are stacked in a puckered plane rather than prefect plane. BP is a direct band gap semiconductor material. The direct band-gap varies with nano-sheet thickness from $\sim$2 eV in monolayer to $\sim$0.3 eV for bulk black phosphorus.[1–3] This is different from another 2D crystal material MoS_2, which only exhibits direct gap in monolayer. The carrier mobility of BP up to 1000 cm^2/V s at room temperature and current on/off ratios reached $\sim$10^4–10^5.[4–6] Due to the small band-gap, both p-type and n-type configurations can be tuned in BP, while few-layer MoS_2 just can be tuned into n-type. Based on those excellent performance, BP has a great potential application in many fields. Considering the adjustable band-gap, BP can be used to produce high-performance field effect transistors;[7] The high electron mobility characteristics can be utilized as electrode-channel contacts material,[8] photodiodes;[9] Additionally, BP shows application prospect in lithium battery manufacturing,[10] gas sensor,[11] thermoelectric device,[12–14] and superior mechanical flexibility.[15]

The thickness-dependent direct band-gap lead to potential applications in extraordinary light emission,[16] and efficient photo-electrical conversion,[17] especially in the infrared regime. In recent years, researchers have paid attention to the optical properties of BP in case of different thickness, various doping conditions, and different polarization directions of the excitation light.[3,8,18] Since previous reports[19–24] have shown that graphene, MoS_2, topological insulators have excellent saturable absorption (SA) properties, all of them are alternative materials for saturation absorbers. As a new member of the 2D crystal material family, BP also shows excellent nonlinear optical properties.[25,26] Damien[27] found that BP materials, prepared by liquid phase exfoliation, exhibit transmittance enhancement with the increase of laser intensity. This result exhibits typical nonlinear characteristic in BP. Compared to other graphene-like 2D materials, tunable optical properties and direct bandgap for all thicknesses of BP may bring significant benefit to various photonics applications.

In this work, the dynamic relaxation process (ultrafast recovery time) was measured by pump-probe experiments at wavelength of 1550 nm for BP suspension. The ultrafast carrier dynamic relaxation time for nonlinear response was obtained by exponential function fitting to the experimental results. Compared with the nonlinear responses of graphene and MoS_2, the nonlinear response and recovery time of BP are much faster. At last, the open aperture (OA) Z-scan experiments were carried out to study the saturable absorption performance at infrared band (1550 nm) and visible band (532 nm and 680 nm). By fitting the experimental data, we obtained the nonlinear absorption coefficients as $\beta_2 = -0.20 \pm 0.08 \times 10^{-3}$ cm/GW (532 nm), $\beta_2 = -0.12 \pm 0.05 \times 10^{-3}$ cm/GW (680 nm), and $\beta_2 = -0.15 \pm 0.09 \times 10^{-3}$ cm/GW (1550 nm).

a)Email: sixiao@csu.edu.cn
b)Email: junhe@csu.edu.cn

The BP crystals were purchased from Smart Elements. The solution-based mechanical exfoliation process started from the mixing of BP crystals with ethanol solution. The final purified BP-ethanol mixture has a concentration ∼6 mg/ml. Atomic force microscopy (AFM) was used to study the thickness and morphology of BP nanoflakes (Agilent 5500); the microstructure of BP was determined by scanning transmission electron microscopy (TEM, JEOL JEM-2100F) operated at 200 kV; the optical transmission spectrum of BP suspension was characterized by UV-Visible spectrophotometer.

The transient dynamic response measurements were performed using a femto-second pulse laser with pulse duration of 35 fs. The femto-second laser pulse was produced by an optical parametric amplifier (TOPAS, USF-UV2), which was pumped by a Ti: Sapphire regenerative amplifier system (Spectra-Physics, Spitfire ACE-35F-2KXP, Maitai SP and Empower 30). The pulse repetition rate is 2 kHz. The laser beam was focused by a lens with focus length of 250 mm. Both the wavelengths of the pump and probe light are chosen as 1550 nm. The nonlinear optical properties of the BP suspension were investigated with the same femto-second laser system. The OA Z-scan experiments were carried out at wavelengths of 1550 nm, 680 nm, and 532 nm, respectively. The laser beam was focused by a lens with focal distance of 150 mm.

Figure 1(a) demonstrates the TEM image for BP nanoflakes. We notice that the size of BP nanoflakes is up to 100 nm. Figure 1(b) shows the AFM images of the BP nanoflakes. The nanoflake thickness ranges from 10 nm to 30 nm. The high resolution TEM image in Figure 1(c) reveals the structures of BP which have the lattice space of 0.217 nm corresponding to (002) facets. As depicted in inset of Figure 1(c), the selective area diffraction (SAED) pattern confirms that BP

have excellent crystallinity. The normalized transmission spectrum of BP suspension is illustrated in Figure 1(d).

Considering the linear optical transmission spectrum, significant absorption peak appears in the vicinity of 1500 nm, which indicates that the samples have interband optical transition energy close to 0.8 eV. Then, according to the previous work,[3,8] BP nanosheets (2–3 monolayers) have a band gap close to 0.8 eV and we can learn that the thickness of the nanosheets is about 10 Å (=1 nm) from the structure diagram, as shown in the inset of Figure 1(a). We may infer that our as-fabricated BP is mainly made up by multi-layer (2–3 monolayers) nanosheets with the thickness of about 1 nm. Finally, we find that the nanosheets are stacked together in terms of further TEM characterization. Meanwhile, AFM characterization showed that the thickness of nanoflakes was ranged from 10 to 30 nm. Thus, we conjecture that such nanosheets composed of 2–3 monolayers mainly stack together to form the nanoflakes (10–30 nanosheets layer).

Figure 2(a) presents carriers dynamic relaxation process for the BP suspension taken at pump and probe wavelength of 1550 nm. The average power of pump light is 0.9 μW. The main figure shows the experimental data with the theoretically fitting curve for a fast relaxation process while the inset schematically illustrates the transient dynamic processes in BP suspension. Dynamic relaxation process exhibits a exponential decay, and it can be fitted by exponential decay function of $y = A_1 e^{-(x-x_0)/\tau_S} + y_0$, where τ_s represents the fast relaxation time during dynamic relaxation and is obtained as $\tau_s = 24 \pm 2$ fs. We believe that this fast decay (τ_s) is correlated to the intra-band relaxation process.[28,29] This ultrafast recovery time (intra-band relaxation time) makes BP a potential material for generating ultrashort pulses.[30,31]
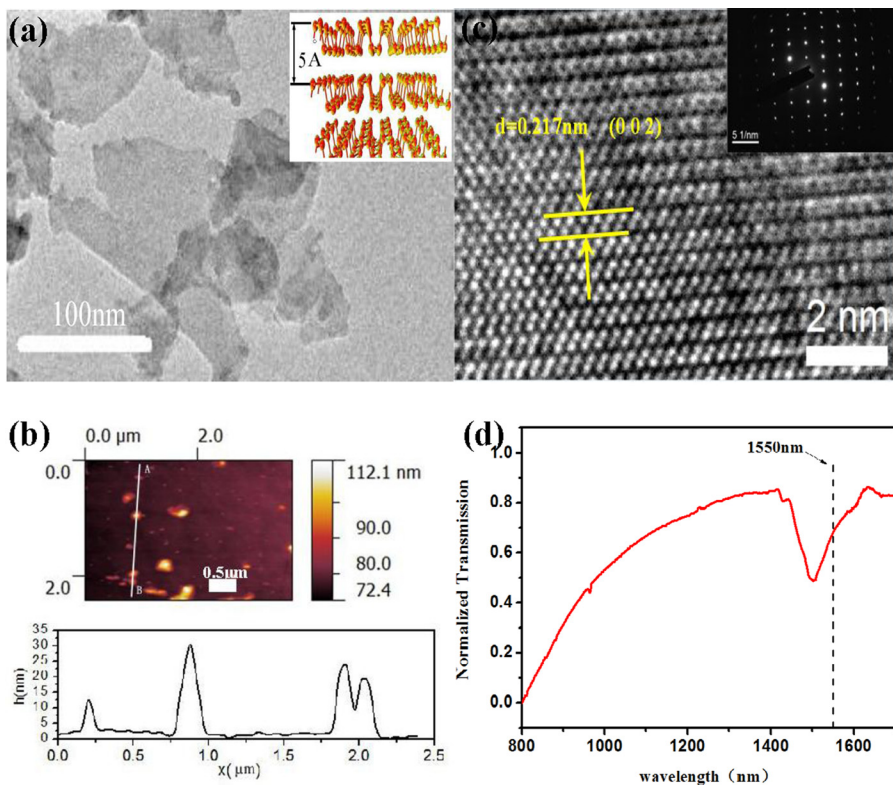

FIG. 1. Material characterizations of BP. (a) TEM image of BP nanoflakes. Scale bar: 100 nm. Inset: lateral view of the atomic structure of BP. (b) AFM image of BP nanoflakes on substrate. Scale bar: 0.5 μm. (c) HRTEM image of BP nanosheet. Inset: SAED pattern. Scale bars are 2 nm and 51 nm^{-1} (inset). (d) Normalized transmission spectrum of BP suspension.
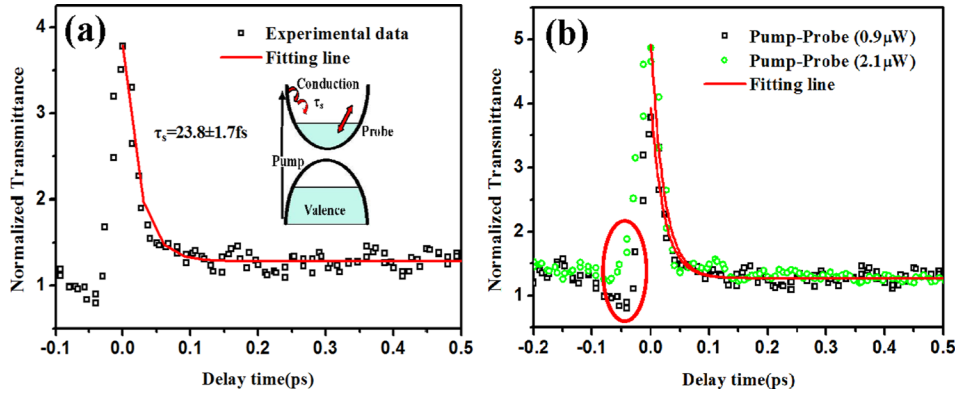
FIG. 2. (a) Fast relaxation dynamics for BP suspension with a pump wavelength of 1550 nm and pump average power of 0.9 μW. The inset schematically illustrates the transient dynamics processes in BP. (b) Fast relaxation dynamics for BP suspension under different pump powers.

Further discussion on the origins of ultrafast recovery time will be presented in the next paragraph.

Carrier relaxation dynamics were compared at wavelength of 1550 nm in different pump average power of 0.9 μW and 2.1 μW, which was depicted in Figure 2(b). According to the exponential fitting of experimental data measured under the larger power of 2.1 μW, the fast relaxation time is determined to ~20 fs, which means that the increase of pump power did not obviously affect the carrier dynamics process. Since we are using the pulse laser with a low repetition rate (2 kHz), the pulse intervals are 0.5 ms. Compared with the femtosecond relaxation time, the thermal effects on nonlinear absorption are negligible. In addition, an interesting experimental phenomenon was observed. During the pump-probe process, the probe transmittance dropped abruptly when the pump-probe delay was near around the zero position under low intensity excitation, which is marked by red ellipse circle in Figure 2(b). Such a phenomenon disappeared when the pump power increased. We guess that the problem of Gaussian beam might induce this abnormal phenomenon. What is more, it reminded us that suitable power may help to convent such abnormal phenomena during similar experiments.

Basically, thermal effects may play a role during the carrier dynamics relaxation process. But it should not play the main role in our experiments. As we know, with the increase of excitation intensity, thermal effect will be more obvious in the sample. That means carrier relaxation dynamics process will become slower at larger pump power which has more thermal accumulation. Nevertheless, no obvious change was observed for the fast dynamics relaxation time when the average power was increased from 0.9 to 2.1 μW, which is shown in Figure 2(b). We conclude that, the electron relaxation rather than thermal dissipation dominates the relaxation dynamics observed in our experiments, which is in agreement with previous reports on MoS$_2$.[29]

Even though the fast carriers dynamic relaxation time may not be precisely determined due to the limit of time resolution(i.e., 35 fs) of the measurement system, the ultrafast relaxation process can still be confirmed by the pump-probe experiments. In Table I, we compared the recovery time (intra-band relaxation time) of graphene, MoS$_2$ (few-layer), MoS$_2$ (thick crystal), and BP. It is not difficult to

find that ultrafast recovery time of BP is dramatically shorter than that of the others. We assigned the fast intra-band relaxation in few-layer BP to defect-assisted carrier cooling. In defect-assisted model,[29,32] relaxation occurs by the following sequential process: An electron makes a transition from the nanocrystal to the defect, the defect relaxes by multi-phonon emission, and the electron makes a second transition to a lower-lying energy level of the nanocrystal. The defect provides a channel for nonradiative intra-band carrier relaxation. As previously described, a puckered honeycomb structure is formed by phosphorus atoms in BP monolayer. Considering the puckered structure, the specific surface area for BP is much larger than that for graphene and MoS$_2$, which have plane structure. Therefore, in the same volume, the quantity of defects in BP may be much larger than that in other 2D materials. Those dislocation vacancies and edges as well as adsorbate would accelerate the intra-band relaxation process through defect-assisted model.

As shown in Figure 3, the nonlinear optical response of BP suspension was investigated at the wavelength of 1550 nm (excitation irradiances: 15 GW/cm^2), 680 nm (39 GW/cm^2), and 532 nm (12 GW/cm^2) by use of OA Z-scans. First, we selected the visible band as the excitation source(532 nm, 680 nm) to study the ultrafast nonlinear optical behavior of the BP suspension. Figures 3(a) and 3(b) demonstrate the OA Z-scan results for 532 nm and 680 nm which demonstrate SA behavior. In Figure 3(c), the saturable absorption effect is also observed at the wavelength of 1550 nm, which is around the linear absorption peak position. The SA properties in BP provide experimental basis for potential application as infrared saturation absorbers.

According to the nonlinear optical theory, based on a spatially and temporally Gaussian pulse, the normalized energy transmittance, $T_{OA}(z)$, is given by[33]

TABLE I. Compare the fast dynamic relaxation time of BP, MoS$_2$, graphene.

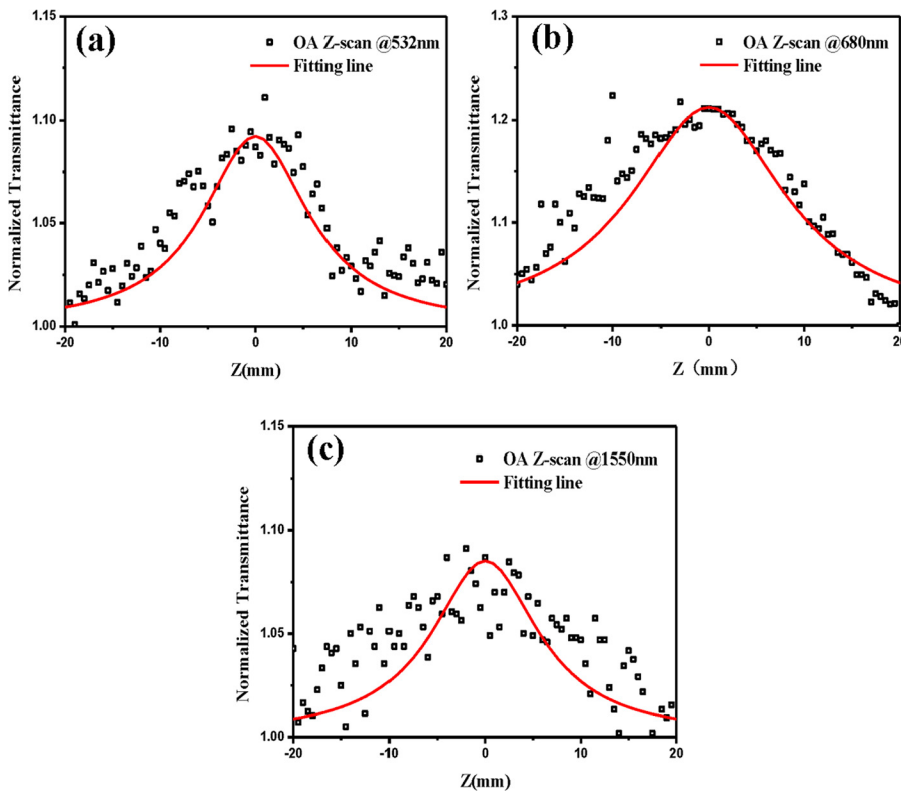| Material	Wavelength (nm)	τ_s	References
BP	1550	24 $\pm$ 2 fs	Present work
MoS$_2$ (few-layer)	670	2.1 $\pm$ 0.1 ps	29
MoS$_2$ (thick crystal)	670	1.8 $\pm$ 0.6 ps	29
Graphene	1600	1.27 $\pm$ 0.12 ps	35
Graphene	(THz pulses)	150 fs	31

FIG. 3. Open-aperture Z-scans of BP suspension at different wavelengths: (a) 532 nm, (b) 680 nm, and (c) 1550 nm.

$$T_{OA}(z) = \frac{1}{\sqrt{\pi}q_0} \int_{-\infty}^{\infty} \ln\left[1+q_0 \exp(-x^2)\right]dx, \quad (1)$$

where $q_0 = \beta_2 I_0 L_{eff}$, β_2 is nonlinear absorption coefficient, $L_{eff} = [1-\exp(-\alpha l)/\alpha]$, α is linear absorption coefficient, and l is the sample path length. β_2 can be extracted by fitting the equation above to the OA Z-scan experimental curves. The contribution of β_2 is only attributed to the nonlinear absorption of the BP, since all measurements were carried out on pure dispersant solvent under the same experimental conditions and no significant nonlinear response was observed. By fitting the OA Z-scan data in Figures 3(a)–3(c) using Eq. (1), we obtained the nonlinear absorption coefficient of $\beta_2 = -0.20 \pm 0.08 \times 10^{-3}$ cm/GW (532 nm), $\beta_2 = -0.12 \pm 0.05 \times 10^{-3}$ cm/GW (680 nm), and $\beta_2 = -0.15 \pm 0.09 \times 10^{-3}$ cm/GW (1550 nm). This negative nonlinear absorption effect shows comparable nonlinear absorption capability with that of MoS_2 nanosheets[17] ($\beta_2 = -4.6 \pm 0.27 \times 10^{-3}$ cm/GW). Additionally, the observed broadband saturable absorption in BP suggests that it can serve as an ultrafast nonlinear saturation absorber, an essential mode locking element for ultrashort pulsed lasers.[22,34] The third-order nonlinear optical susceptibility, $Im\chi^3$, and the figure of merit (FOM) require a further study, which is currently under the way.

In conclusion, the ultrafast relaxation dynamics and excellent broadband saturable absorption properties of BP suspension have been studied by use of pump-probe and Z-scan techniques. The ultrafast recovery time in BP was determined to be ~24 fs, which is much faster than that of previous 2D crystal materials. The OA Z-scan experiments demonstrates that BP has perfect saturable absorption performance at both infrared band (1550 nm) and visible band (532 nm and 680 nm). The nonlinear absorption coefficients

were obtained as $\beta_2 = -0.20 \pm 0.08 \times 10^{-3}$ cm/GW (532 nm), $\beta_2 = -0.12 \pm 0.05 \times 10^{-3}$ cm/GW (680 nm), and $\beta_2 = -0.15 \pm 0.09 \times 10^{-3}$ cm/GW (1550 nm), respectively. We believe that the excellent nonlinear optical properties will make BP a preferred alternative material for saturable absorbers.

[1]Y. Takao and A. Morita, Physica B&C **105**, 93 (1981).
[2]R. W. Keyes, Phys. Rev. **92**, 580 (1953).
[3]A. S. Rodin, A. Carvalho, and A. H. Neto Castro, Phys. Rev. Let. **112**, 176801 (2014).
[4]H. Liu, A. T. Neal, Z. Zhu, Z. Luo, X. Xu, D. Tomanek, and P. D. Ye, ACS Nano **8**, 4033 (2014).
[5]P. K. Steven, A. D. Rostislav, S. Hennrik, A. H. C. Neto, and B. Ozyilma, Appl. Phys. Lett. **104**, 103106 (2014).
[6]A. D. Rostislav, P. K. Steven, Y. Yeo, K. Watanabe, T. Taniguchi, and B. Ozyilmaz, Appl. Phys. Lett. **106**, 083505 (2015).
[7]L. Li, Y. Yu, G. J. Ye, Q. Ge, X. Ou, H. Wu, D. Feng, X. H. Chen, and Y. Zhang, Nat. Nanotechnol. **9**, 372 (2014).
[8]J. S. Qiao, X. H. Kong, Z. X. Hu, F. Yang, and W. Ji, Nat. Commun. **5**, 4475 (2014).
[9]G. Pascal, U. Roberto, L. D. Dinh, B. Marko, and K. Klaus, Appl. Phys. Lett. **106**, 233110 (2015).
[10]J. Sun, G. Zheng, H. W. Lee, N. Liu, H. Wang, H. Yao, W. Yang, and Y. Cui, Nano Lett. **14**, 4573 (2014).
[11]L. Kou, T. Frauenheim, and C. Chen, J. Phys. Chem. Lett. **5**, 2675 (2014).
[12]H. Y. Lv, W. J. Lu, D. F. Shao, and Y. P. Sun, Phys. Rev. B. **90**, 085433 (2014).
[13]R. X. Fei, A. Faghaninia, R. Soklaski, J. A. Yan, C. Lo, and L. Yang, Nano Lett. **14**, 6393 (2014).

[14]E. Flores, J. R. Ares, A. Castellanos-Gomez, M. Barawi, I. J. Ferrer, and C. Sanchez, Appl. Phys. Lett. **106**, 022102 (2015).

[15]Q. Wei and X. H. Peng, Appl. Phys. Lett. **104**, 251915 (2014).

[16]S. Zhang, J. Yang, R. Xu, F. Wang, W. Li, M. Ghufran, Y. W. Zhang, Z. Yu, G. Zhang, Q. Qin, and Y. Lu, ACS Nano **8**, 9590 (2014).

[17]H. Yuan, X. Liu, F. Afshinmanesh, W. Li, G. Xu, J. Sun, B. Lian, G. Ye, Y. Hikita, and Z. Shen, preprint arXiv:1409.4729 (2015).

[18]T. Low, A. Rodin, A. Carvalho, Y. Jiang, H. Wang, F. Xia, and A. C. Neto, Phys. Rev. B **90**, 075434 (2014).

[19]Q. L. Bao, H. Zhang, Z. H. Ni, Y. Wang, L. Polavarapu, Z. X. Shen, Q. H. Xu, and D. Y. Tang, Nano Res. **4**, 297 (2011).

[20]X. Y. He, Z. B. Liu, D. N. Wang, M. W. Yang, T. Y. Hu, and J. G. Tian, Photonics. Technol. Lett. **25**, 1392 (2013).

[21]H. Zhang, S. B. Lu, J. Zheng, J. Du, S. C. Wen, D. Y. Tang, and K. P. Loh, Opt. Express **22**, 7249 (2014).

[22]K. Wang, J. Wang, J. Fan, M. Lotya, A. O'Neill, D. Fox, Y. Feng, X. Zhang, B. Jiang, Q. Zhao, H. Zhang, J. N. Coleman, L. Zhang, and W. J. Blau, ACS Nano **7**, 9260 (2013).

[23]S. B. Lu, C. J. Zhao, Y. H. Zou, S. Q. Chen, Y. Chen, Y. Li, H. Zhang, S. C. Wen, and D. Y. Tang, Opt. Express **21**, 2072 (2013).

[24]S. Q. Chen, C. J. Zhao, Y. Li, H. H. Huang, S. B. Lu, H. Zhang, and S. C. Wen, Opt. Mater. Express **4**, 587 (2014).

[25]S. B. Lu, L. L. Miao, Z. N. Guo, X. Qi, C. J. Zhao, H. Zhang, S. C. Wen, D. Y. Tang, and D. Y. Fan, Opt. Express **23**, 11183 (2015).

[26]Y. Chen, G. B. Jiang, S. Q. Chen, Z. N. Guo, X. F. Yu, C. J. Zhao, H. Zhang, Q. L. Bao, S. C. Wen, D. Y. Tang, and D. Y. Fan, Opt. Express **23**, 12823 (2015).

[27]D. Hanlon, C. Backes, E. Doherty, C. S. Cucinotta, N. C. Berner, C. Boland, K. Lee, P. Lynch, Z. Gholamvand, and A. Harvey, e-print arXiv:1501.01881 (2015).

[28]H. Shi, R. Yan, S. Bertolazzi, J. Brivio, B. Gao, A. Kis, D. Jena, H. G. Xing, and L. Huang, ACS Nano **7**, 1072 (2013).

[29]Q. Wang, S. Ge, X. Li, J. Qiu, Y. Ji, J. Feng, and D. Sun, ACS Nano **7**, 11087 (2013).

[30]Q. L. Bao and K. P. Loh, ACS Nano **6**, 3677 (2012).

[31]P. A. George, S. Jared, D. Jahan, S. Shriram, C. Mvs, R. Farhan, and G. S. Michael, Nano Lett. **8**, 4248 (2008).

[32]F. S. Darrell and J. G. David, Phys. Rev. B **54**, 1486 (1996).

[33]R. L. Sutherland, *Handbook of Nonlinear Optics*, 2nd ed. (Marcel Dekker, New York, 2003).

[34]W. J. Blau and J. Wang, Nat. Nanotechnol. **3**, 705 (2008).

[35]A. E. Nikolaenko1, N. Papasimakis1, E. Atmatzakis1, Z. Luo, Z. X. Shen, F. D. Angelis, S. A. Boden, E. D. Fabrizio, and N. I. Zheludev, Appl. Phys. Lett. **100**, 181109 (2012).